Synthesis and Characterization of Boron-Containing Ferrocenyl Ligands for Asymmetric Catalysis

Barbara F. M. Kimmich, Clark R. Landis,* and Douglas R. Powell

Department of Chemistry, University of Wisconsin−Madison, 1101 University Avenue, Madison, Wisconsin 53706

Received June 4, 1996[⊗]

Novel boronato-functionalized ferrocenylphosphine ligands **3a**−**c** have been synthesized from (*S*,*R*)-1,1′-bis(diphenylphosphino)-2-[1((1-hydroxy-2-phenyl)amino)ethyl]−ferrocene (**2**). These ligands form stable ligand−metal adducts with Rh(I) complexes that are catalytically active in hydrogenation and hydroformylation reactions. The square-planar metal complex Pt(**2**)(Me)I exhibits a structure that appears well-suited to support secondary interactions between the Lewis acidic boron functionality and Lewis basic sites of functionalized, coordinated alkenes.

Introduction

Tremendous progress has been made in the development of highly selective and active homogeneous transition-metal catalysts.[1] Many catalysts, e.g. those that employ chiral bidentate ligands such as BINAP[2] and DuPHOS,[3] impart enantioselectivity through steric interactions between a substrate and the coordinated ligand. Recently, Ito has coined the term "secondary interactions" to describe catalysts that control selectivity via weak bonding interactions between the substrate and the ligand.[4] These attractive catalyst−substrate interactions occur outside the metal's primary coordination sphere and may include electrostatic interactions,[5] hydrogen bonding,[6] and Lewis acid−base interactions.[7] The identification of ligand structures that can predictably place functional groups in the proximity of their substrate-based complements is critical to developing the control of selectivity via secondary interactions. In this paper we report progress in the construction of ligand frameworks that may lead to catalytically useful secondary interactions.

Two criteria to be satisfied in designing ligands that impart selectivity via secondary interactions are (1) the framework of the ligand must allow secondary interactions without prohibitive strain, leading to a reaction transition state which is stabilized with respect to undesired reaction pathways, and (2) the secondary interaction must be formed rapidly and reversibly. Our tactile and computer-generated modeling studies indicate that the ferrocenyl bis(phosphine) backbone provides a rigid framework which can orient the secondary interaction over an open coordination site of a catalytic metal center.[8] This widely used class of ligands is derivatized readily, making possible a wide variety of different secondary interactions.[6,9] In this paper we focus on the attachment of boronato groups to the diphosphine ligands. These functional groups are weak Lewis acids that are known to reversibly bind Lewis bases such as amines (Figure 1a).[10] Additionally, borates and aminoborates rapidly transesterify and transamidify with alcohols and amines,[11] respectively, making them prime candidates for covalent secondary interactions (Figure 1b). Herein we report the preparation, spectroscopic and structural characterization, and catalytic properties of metal complexes of the novel boron-containing ligands **3a**−**c**.

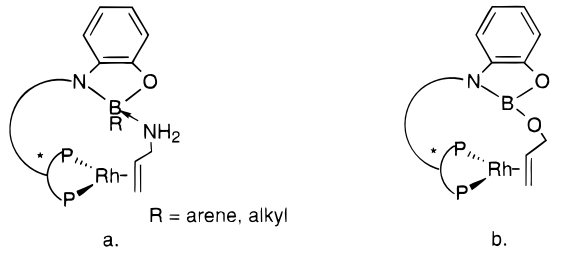

Figure 1. (a) Proposed Lewis acid−base secondary interaction. (b) Proposed covalent secondary interaction.

Results and Discussion

(*S*,*R*)-1,1′-Bis(diphenylphosphino)-2-(1-acetoxyethyl)-ferrocene (**1**; (*S*,*R*)-BPPFAc) is a useful starting material for making chiral substituted bis(phosphine) ferrocenyl ligands.[9] By a procedure similar to that used by Ito and co-workers[9] (*S*,*R*)-1,1′-bis(diphenylphosphino)-2-[1-((1-hydroxy-2-phenyl)amino)ethyl]ferrocene (**2**; (*S*,*R*)-BPPFAP) formed when **1** was refluxed in toluene with a large excess of 2-aminophenol for 18 h (Scheme 1). The

[⊗] Abstract published in *Advance ACS Abstracts,* September 1, 1996.

(1) For reviews see: (a) Ojima, L.; Clos, N.; Bastos, C. *Tetrahedron* **1989**, *45*, 6901. (b) Noyori, R.; Kitamura, M. In *Modern Synthetic Methods*; Scheffold, R., Ed.; Springer-Verlag: Berlin, 1989; Vol. 5, p 115.

(2) Miijashita, K.; Yasuda, A.; Takaya, H.; Toriumi, K.; Ito, T.; Souchi, T.; Noyori, R. *J. Am. Chem. Soc.* **1982**, *102*, 7932.

(3) Burk, M. J.; Feaster, J. E.; Harlow, R. L. *Organometallics* **1990**, *9*, 2653.

(4) Sawamura, M.; Ito, Y. *Chem. Rev.* **1992**, *92*, 857.

(5) Sawamura, M.; Nagata, H.; Sakamoto, H.; Ito, Y. *J. Am. Chem. Soc.* **1992**, *114*, 2586.

(6) Hayashi, T.; Kanehira, K.; Hagihara, T.; Kumada, M. *J. Org. Chem.* **1988**, *53*, 113.

(7) (a) Börner, A.; Ward, J.; Kortus, K.; Kagan, H. B. *Tetrahedron. Asymmetry* **1993**, *4*, 2219. (b) Fields, L. B.; Jacobsen, E. N. *Tetrahedron. Asymmetry* **1993**, *4*, 2229.

(8) Cleveland, T.; Landis, C. R. Unpublished results.

(9) Hayashi, T.; Mise, T.; Fukushima, M.; Kagotani, M.; Nagashima, N.; Hamada, Y.; Matsumoto, A.; Kawakami, S.; Konishi, M.; Yamamoto, K.; Kumada, M. *Bull. Chem. Soc. Jpn.* **1980**, *53*, 1138 and references cited therein.

(10) (a) Toyota, S; Oki, M. *Bull. Chem. Soc. Jpn.* **1990**, *63*, 1168. (b) Narasaka, K.; Sakurai, H.; Kato, T.; Iwasawa, N. *Chem. Lett.* **1990**, 1271.

(11) Brauch, T. W.; Landis, C. R. Unpublished results.

S0276-7333(96)00447-5 CCC: $12.00

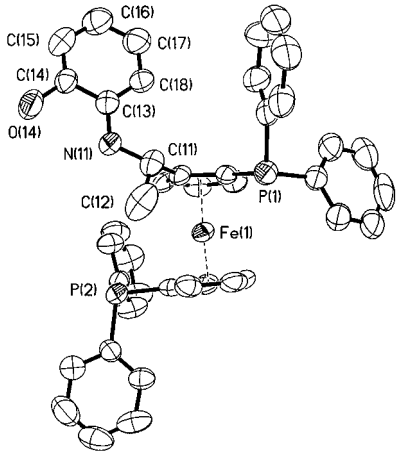

Figure 2. X-ray crystal structure for *rac*-BPPFAP (**2**). The displacement ellipsoids are drawn at 35% probability. Hydrogens have been removed for clarity. Selected bond lengths (Å) and bond angles (deg): N(11)−C(11), 1.454(10); N(11)−C(13), 1.389(10); O(14)−C(14), 1.385(9); N(11)−C(13)−C(14), 118.5(7); O(14)−C(14)−C(13), 114.9(8).

Scheme 1

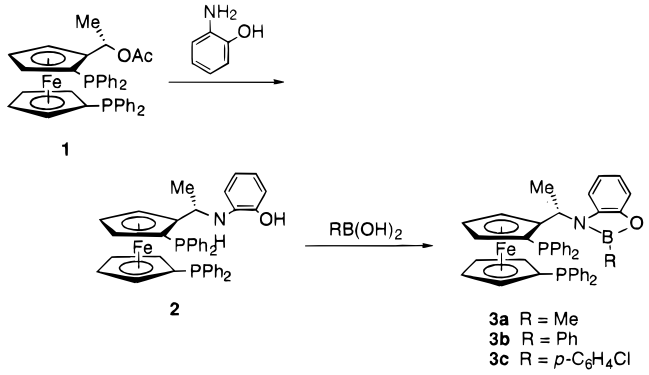

^{1}H and ^{31}P NMR and liquid secondary ion mass spectrometry (LSIMS) spectra and the X-ray crystallographic structure (Figure 2) are all consistent with the formulation of (*S*,*R*)-BPPFAP. The overall structural characteristics of BPPFAP are similar to those of 1-[(*R*)-1′,2-bis(diphenylphosphino)ferrocenyl]-(*S*)-*N*,*N*-dimethylethylamine.[12]

(*S*,*R*)-BPPFAP (**2**) was reacted with a series of boric acid derivatives using a procedure based on the work of Fields and Jacobsen (Scheme 1).[7b] The resulting boron-containing ferrocenyl ligands (*S*,*R*)-**3a**−**c** (BPPFAP-BMe, BPPFAP-BPh, and BPPFAP-BPhCl, respectively) as solids were handled in air with no apparent decomposition. The crystal structure of *rac*-**3a** is shown in Figure 3 (see Table 1 for selected bond lengths and angles).

Ligands **2** and **3a**−**c** form stable metal complexes. Reaction of the boronate ligands **3a**−**c** with $PtMe_2$(COD) (COD = cyclooctadiene) in benzene at 60 °C yielded the complexes **4a**−**c** (Scheme 2). Formation of the platinum complexes was supported by the characteristic Pt coupling pattern in ^{31}P NMR spectra,[13] the appearance of inequivalent Pt−Me and free cyclooctadiene resonances in ^{1}H NMR spectra, and the mass spectral data. LSIMS spectra reveal weak peaks corresponding to parent ions

(12) Shawkataly, O. B.; Fun, H.-K.; Chinnakali, K.; Yip, B.-C.; Teoh, S.-G.; Ito, Y.; Sawamura, M. *Acta Crystallogr.* **1993**, *C49*, 139.

(13) ^{195}Pt is 33.8% abundant ($I = {}^1/_2$) and yields a characteristic satellite pattern which looks like a triplet.

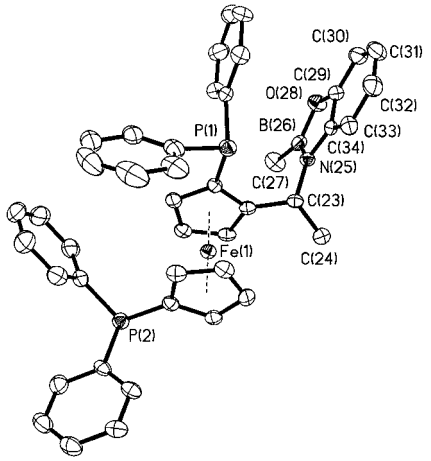

Figure 3. X-ray crystal structure for *rac*-BPPFAP-BMe (**3a**). The displacement ellipsoids are drawn at 50% probability. The solvent molecule and hydrogens have been removed for clarity.

Table 1. Selected Bond Lengths (Å) and Angles (deg) for *rac*-BPPFAP-BMe (3a)

Bond Lengths			
C(23)−N(25)	1.486(5)	B(26)−C(27)	1.564(7)
N(25)−C(34)	1.403(5)	B(26)−O(28)	1.415(6)
N(25)−B(26)	1.428(6)	O(28)−C(29)	1.380(5)
Bond Angles			
C(34)−N(25)−C(23)	123.3(3)	O(28)−B(26)−N(25)	108.0(4)
C(34)−N(25)−B(26)	107.4(3)	O(28)−N(25)−C(27)	121.9(4)
B(26)−N(25)−C(23)	129.5(4)	C(29)−O(28)−B(26)	107.2(3)
N(25)−B(26)−C(27)	130.2(4)		

Scheme 2

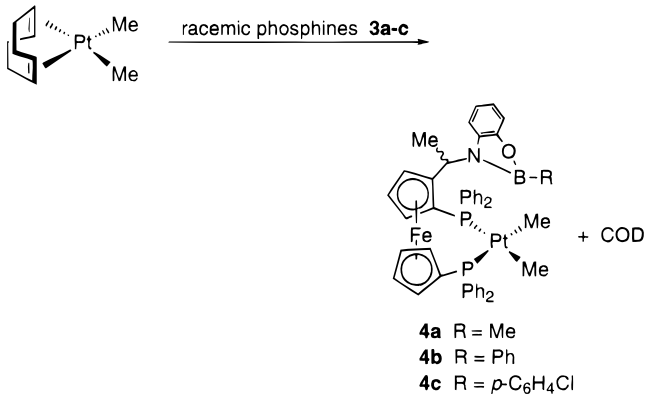

of **4b** and **4c** and strong peaks for ions generated by the loss of one methyl group for **4a**−**c**.

rac-BPPFAP (**2**) reacted with $PtMe_2$(COD) to give a single product which exhibits ^{31}P NMR resonances similar to those for complexes **4a**−**c**. However, this complex slowly decomposed in solution, presumably via methane loss due to protonolysis of the Pt−Me bond by the weakly acidic phenol. The reaction of *rac*-BPPFAP with PtMeI(COD) yielded the stable complex PtMeI(**2**), which is far less susceptible to loss of the methyl group than $PtMe_2$(BPPFAP) (Scheme 3). Because the phosphines are inequivalent, two geometric isomers are possible. In solution both isomers, **5a** and **5b**, are present approximately in a 1:1 ratio, as revealed by NMR spectra. The crystal characterized by X-ray crystallography comprised a mixture of isomers (Figure 4, Table 2) in a 30:70 ratio (**5a**:**5b**). The two phosphorus atoms coordinate to platinum, occupying cis sites in a distorted-square-planar geometry. The environment of

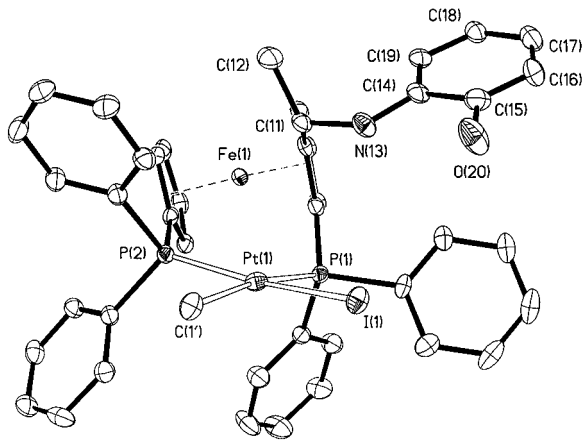

Figure 4. X-ray crystal structure for PtMeI(*rac*-BPPFAP) (**5b**). The displacement ellipsoids are drawn at 50% probability. The acetone molecule and all hydrogens have been removed for clarity. The methyl and iodide groups attached to the platinum were disordered. Isomer **5b** had an occupancy of 0.7299(12).

Scheme 3

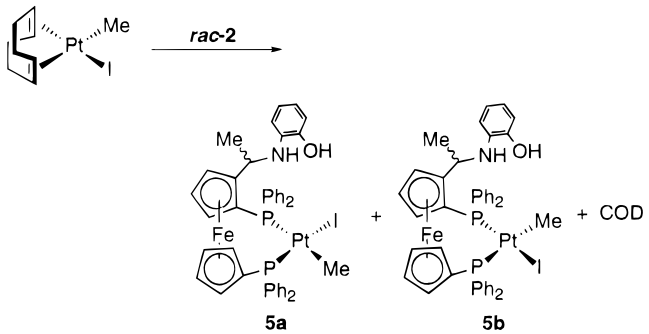

Table 2. Selected Bond Lengths (Å) and Bond Angles (deg) for PtMeI(*rac*-BPPFAP) (5b)

Bond Lengths			
Pt(1)−C(1′)	2.163(7)	N(13)−C(14)	1.384(6)
Pt(1)−I(1)	2.5989(4)	O(20)−C(15)	1.367(6)
P(1)−Pt(1)	2.3215(10)	I(1)−N(13)	4.008(2)
P(2)−Pt(1)	2.2737(10)	I(1)−O(20)	3.968(2)
N(13)−C(11)	1.467(5)		
Bond Angles			
(C1′)−Pt(1)−I(1)	85.8(2)	N(13)−C(14)−C(15)	116.7(4)
P(1)−Pt(1)−P(2)	97.90(4)	O(20)−C(15)−C(14)	115.2(4)
P(1)−Pt(1)−I(1)	92.80(3)	I(1)−N(13)−Pt(1)	69.9(6)
P(2)−Pt(1)−C(1′)	84.8(2)	I(1)−O(20)− Pt(1)	108.4(6)

the platinum and phosphorus atoms is quite similar to that of other bis(diphenylphosphino)ferrocene−platinum complexes.[14] For example, $PtCl_2$(dppf) (dppf = bis(diphenylphosphino)ferrocene) has Pt−P bond lengths (2.252(4) and 2.260(4) Å) similar to those of complex **5b** (2.3215(10) and 2.2737(10) Å).[14a]

Significantly, the crystallographic structure of **5a** reveals a proximal relationship between the aminophenol functional group and the metal coordination sites. The O and N atoms of the aminophenol each are located 4.0 Å (Table 2) above the coordinated iodide in a direction approximately perpendicular to the square plane about the Pt. Preliminary molecular mechanics

Table 3. Hydrogenation of Methyl (*Z*)-α-Acetamidocinnamate (MAC)

ligand	initial turnover freq (turnovers/min)	% ee
1	120	9
2	138	54
3a	149	39
3b	22	49
3c	127	53

modeling using the UFF force field suggested that the overall ligand structure is hardly perturbed upon attachment of boron to the aminophenol. Furthermore, modeling studies suggested that such a structure is capable of supporting either Lewis acid−base or covalent bonding between the boron and allylamine or allyl alcohol, respectively.

It is interesting to note that **5a** shares some of the structural characteristics of [Pd(η^3-allyl)(**6**)]ClO_4, a highly selective catalyst for asymmetric allylic amination.[15] In

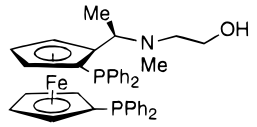

6

the structure of [Pd(η^3-allyl)(**6**)]ClO_4, the pendant side chain on the ferrocenylphosphine ligand is directed toward the reaction site on palladium. The terminal hydroxyl group is located at a position close to one of the π-allyl carbon atoms (3.36(1) Å compared to a distance of 5.24(1) Å from the other carbon). This structural evidence supports Ito and co-workers' proposal that the high selectivity of this catalyst correlates with interaction of the terminal hydroxyl and the incoming amine, thus directing the nucleophilic attack at one of the π-allyl carbons.

Ligands **1**, **2**, and **3a** reacted also with [Rh(NBD)$_2$]OTf (NBD = norbornadiene, OTf = trifluoromethanesulfonate) in acetone to yield the corresponding (*S*,*R*)-[Rh(NBD)(L)]OTf complexes, **7**−**9**. These complexes were isolated as orange-red solids and were characterized by ^{1}H NMR, ^{31}P NMR, and LSIMS. Similar complexes are formed for ligands **3b**,**c**, as indicated by ^{31}P NMR. These complexes, however, could not be isolated as pure materials and slowly decomposed over time in solution into unknown species ($t_{1/2} \approx 3$ days).

Successful hydrogenation and hydroformylation of simple substrates established the catalytic competency of complexes containing the ligands **1**−**3**. All five ligands catalyzed the hydrogenation of MAC, methyl (*Z*)-α-acetamidocinnamate (Table 3). For reasons that are unclear, ligand **3b** yielded a significantly slower catalyst. In keeping with previous results for the hydrogenation of MAC catalyzed by Rh complexes of ferrocene-derived bis(phosphines), unremarkarble enantiomeric excesses (<55% ee) were observed.[16]

Styrene hydroformylation catalyzed by Rh(acac)$(CO)_2$ in the presence of 4 equiv of the ligands **1**−**3** at 80 °C and 90 psig of syngas proceeded slowly (ca. 10 turnovers/h) to yield both normal and internal aldehydes. The

(14) (a) Clemente, D. A.; Pilloni, G.; Corain, B.; Longato, B.; Tiripicchio-Camellini, M. *Inorg. Chim. Acta* **1986**, *155*, L9. (b) Bandoli, G.; Trovó, G.; Dolmella, A.; Longato, B. *Inorg. Chem.* **1992**, *31*, 45. (c) Vasapollo, G.; Toniolo, L.; Cavinato, G.; Bigoli, F.; Lanfranchi, M.; Pellinghelli, A. *J. Organomet. Chem.* **1994**, *481*, 173.

(15) Hayashi, T.; Yamamoto, A.; Ito, Y.; Nishioka, E.; Miura, H.; Yanagi, K. *J. Am. Chem. Soc.* **1989**, *111*, 6301.

(16) Yamamoto, K.; Wakatsuki. J.; Sugimoto, R. *Bull. Chem. Soc. Jpn.* **1980**, *53*, 1132.

Table 4. Crystallographic Data for 2, 3a, and 5

	2	3a	5
formula	$C_{42}H_{37}FeNOP_2$	$C_{43}H_{38}BFeNOP_2$	$C_{43}H_{40}NOP_2FeIPt\cdot C_4H_{10}O$
fw	689.52	713.34	1100.66
cryst color, habit	orange transparent prism	yellow transparent prism	red transparent prism
cryst size, mm	0.50 × 0.40 × 0.20	0.30 × 0.10 × 0.10	0.40 × 0.20 × 0.20
cryst syst	monoclinic	monoclinic	monoclinic
space group	$P2_1/c$; No. 14	$P2_1/n$; No. 14	$P2_1/c$; No. 14
a, Å	14.496(2)	7.1217(2)	13.9080(2)
b, Å	13.560(2)	21.8858(8)	15.9960(2)
c, Å	17.734(3)	23.1841(8)	19.0270(2)
β, deg	97.124(12)	96.851	91.815(2)
V, Å^3	3459.0(9)	3587.8(2)	4230.86(9)
Z	4	4	4
ρ_{calc}, g cm^{-3}	1.324	1.321	1.728
T, K	296(2)	133(2)	133(2)
F(000)	1440	1488	2168
radiation; λ, Å	Mo Kα; 0.710 73	Mo Kα; 0.710 73	Mo Kα; 0.710 73
diffractometer	Siemens P4	Siemens P4/CCD	Siemens P4/CCD
2θ(max), deg	45.0	51.8	52.1
no. of rflns collected	9419	13 693	16 594
no. of rflns used	4495	6206	7377
no. of params refined	424	442	504
$R(F)$, obsd data	0.070	0.061	0.027
$R_w(F^2)$, all data	0.214	0.135	0.076
goodness of fit on F^2	1.194	1.272	1.178

regioselectivity of the hydroformylation varied slightly with ligand (i:n ≈ 2 for ligand **1** and i:n ≈ 4 for **2**, **3a**−**c**). Unusual results are not expected for the hydroformylation of a simple substrate such as styrene.[17] Importantly, these hydrogenation and hydroformylation results clearly demonstrate that these ligands yield active catalysts when combined with common catalyst precursors.

Conclusions

We have prepared and characterized a new class of boron-containing ligands for asymmetric catalysis. These ligands have been shown to catalyze the hydrogenation and hydroformylation of simple substrates. Modeling studies of the crystal structure of **5** indicate that the BPPFAP template is well-suited for the design of new asymmetric ligands for use in catalysis employing secondary interactions. Our future work will focus on the application of the covalent and Lewis acid−base secondary interactions (Figure 1) to catalytic processes such as hydrogenation and hydroformylation.

Experimental Section

General Procedures. All manipulations of water- or air-sensitive compounds were carried out under an atmosphere of nitrogen either by using standard Schlenk techniques or a Braun vacuum glovebox. Glassware was oven-dried before use. All solvents were distilled under nitrogen. Diethyl ether, tetrahydrofuran, benzene, toluene, and hexane were freshly distilled from sodium/benzophenone ketyl. Chloroform-*d* was distilled from P_2O_5, benzene-d_6 was distilled from $LiAlH_4$, and acetone-d_6 was used without purification. ^{1}H NMR (300 MHz) and ^{31}P{^{1}H} NMR (121 MHz) were performed on a Bruker AC-300 spectrometer. All GC runs were performed on an HP 5890A gas chromatograph using Alltech Chirasil-Val and HP Methyl Silicone columns. The ^{1}H spectra were referenced to $SiMe_4$, and the ^{31}P spectra were referenced to H_3PO_4. Low-resolution mass spectra (LR LSIMS) were recorded with a VG AutoSpec spectrometer at a resolution of 2000 using 2-nitrophenyl octyl ether as the matrix. Optical rotations were measured on a Perkin-Elmer 241 polarimeter. Elemental analyses were performed by Desert Analytics Laboratory.

(*S,R*)-BPPFAP (2). The preparation of (*S,R*)-BPPFAP was based on procedures by Hayashi and co-workers.[6,9] (*S,R*)-BPPFAc[9] (**1**; 630 mg, 0.983 mmol) and 2-aminophenol (10 g, 91.6 mmol, 93 equiv) were placed in a Schlenk flask under N_2. Freshly distilled and degassed toluene (60 mL) was added, and the mixture was refluxed for 18 h. The reaction was approximately 95% complete by ^{31}P NMR, and further heating did not improve the yield. Saturated saline solution was cannulated into the reaction mixture. The toluene layer was removed, and the aqueous layer was extracted with toluene (3 × 20 mL). The toluene layer and extracts were dried over Na_2SO_4. Solvent was removed in vacuo, yielding an orange foam. The solid was recrystallized several times from THF/hexane (511 mg, 0.742 mmol, 75% yield). Anal. Calcd for $C_{42}H_{37}NOP_2Fe$: C, 73.15; H, 5.41; N, 2.03; P, 8.98; Fe: 8.10. Found: C, 72.91; H, 5.57; N, 2.05; P, 6.58; Fe, 7.99. $[\alpha]_D$ = +314 ($CHCl_3$, c = 0.42; lit.[9] value for (*R,S*)-BPPFAc (**1**) $[\alpha]_D$ = −314 ($CHCl_3$, c = 0.50)). ^{1}H NMR ($CDCl_3$): δ 1.2 (d, J = 7 Hz, 3H, $CHCH_3$), 3.5−4.3 (m, 7, $C_5H_3FeC_5H_4$), 4.4 (q, J = 7 Hz, 1H, $CHCH_3$), 6.6−6.7 (m, 4, C_6H_4NO), 7.0−7.4 ppm (m, 20H, PC_6H_5). ^{31}P NMR ($CDCl_3$): δ −17.2 (s, PC_5H_4), −23.8 ppm (s, PC_5H_3). LR LSIMS: M^+ at m/e 689.1.

Structure Determination of *rac*-2. A single crystal was grown from THF/hexane at 0 °C. Crystal data are summarized in Table 4.

A total of 9419 reflections with 2θ < 45° were collected on a Siemens P4 diffractometer using graphite-monochromated Mo Kα radiation. The structure was solved by direct methods using the SHELXS-86 program.[18] The structure was refined by full-matrix least squares on F^2 values with hydrogens riding.[19] Non-hydrogen atoms were refined with anisotropic thermal parameters. The final $R(F)$ and $R_w(F^2)$ factors were 0.070 and 0.214, respectively. A molecular structure is shown in Figure 2, along with a partial numbering scheme along with selected bond lengths and bond angles. Fractional coordinates and additional crystallographic data can be found in the Supporting Information.

(*S,R*)-BPPFAP-BMe (3a). The procedure for preparation of **3a** was adapted from procedures by Fields and Jacobsen:[7b] (*S,R*)-BPPFAP (400 mg, 0.58 mmol) and methylboric acid (220 mg, 3.7 mmol, 6.3 equiv) were placed in a Schlenk flask under

(17) Hughes, O. R.; Unruh, J. D. *J. Mol. Catal.* **1981**, *12*, 71.

(18) Sheldrick, G. M. *Acta Crystallogr.* **1990**, *A46*, 467.

(19) Sheldrick, G. M. *SHELXTL VERSION 5 Software Manual*; Siemens Analytical X-ray Instruments: Madison, WI, 1995.

N_2; 50 mL of freshly distilled and degassed benzene was added. The solution was warmed to 50 °C, and the solvent was slowly removed in vacuo. This procedure was repeated two times with an additional 100 mL of benzene. The resulting foam was dissolved in ether and filtered. The crude product was recrystallized several times from diethyl ether (315 mg, 0.442 mmol, 76% yield). Anal. Calcd for $C_{43}H_{38}BNOP_2Fe$: C, 72.40; H, 5.37; B, 1.52; N, 1.96; P, 8.68; Fe, 7.83. Found: C, 71.19; H, 5.41; B, <0.67; N, 1.92; P, 5.31; Fe, 6.87. $[\alpha]_D = +338$ ($CHCl_3$, $c = 0.36$). ^{1}H NMR ($CDCl_3$): δ 0.5 (s, 3H, BCH_3), 1.6 (d, $J = 7$ Hz, 3H, CHCH_3), 3.5−4.7 (m, 7H, $C_5H_3FeC_5H_4$), 5.3 (q, $J = 7$ Hz, 1H, CHCH$_3$), 6.4−7.3 ppm (m, 24H, C_6H_4NO and PC_6H_5). ^{31}P NMR ($CDCl_3$): δ −24.6 (s, C_5H_3P), −17.3 ppm (s, C_5H_4P). LR LSIMS: M^+ at *m/e* 713.3.

Structure Determination of *rac*-3a. A single crystal was grown from slow evaporation of a diethyl ether solution of *rac*-**3a** at room temperature. Crystal data are summarized in Table 4.

A total of 13 693 reflections with $2\theta < 51.8°$ were collected on a Siemens P4/CCD diffractometer using graphite-monochromated Mo Kα radiation.[20] The structure was solved by direct methods and was refined by full-matrix least squares on F^2 values with hydrogens riding.[19] Non-hydrogen atoms were refined with anisotropic thermal parameters. The final $R(F)$ and $R_w(F^2)$ factors were 0.061 and 0.135, respectively. A molecular structure is shown in Figure 3, along with a partial numbering scheme. Selected bond lengths and bond angles are given in Table 1. Fractional coordinates and additional crystallographic data can be found the Supporting Information.

(*S,R*)-BPPFAP-BPh (3b). (*S,R*)-BPPFAP (198 mg, 0.287 mmol) and phenyl boric acid (230 mg, 1.89 mmol, 6.5 equiv) were reacted as above. The crude product was purified by repeated recrystallization from diethyl ether (181 mg, 0.23 mmol, 80% yield). Anal. Calcd for: $C_{48}H_{40}BNOP_2Fe$: C, 74.35; H, 5.20; N, 1.81; P, 7.99; Fe, 7.20. Found: C, 73.44; H, 6.19; N, 1.87; P, 5.96; Fe, 7.07. $[\alpha]_D = +267$ ($CHCl_3$, $c = 0.40$). ^{1}H NMR ($CDCl_3$): δ 1.9 (d, $J = 7$ Hz, 3H, CHCH_3), 3.5−5.0 (7 peaks, m, 7H, $C_5H_3FeC_5H_4$), 6.0 (q, $J = 7$ Hz, 1H, CHCH$_3$), 6.4−7.9 ppm (m, 29H, BC_6H_5, C_6H_4 and PC_6H_5). ^{31}P NMR ($CDCl_3$): δ −25.6 (s, C_5H_3P), −17.4 ppm (s, C_5H_4P). LR LSIMS: M^+ at *m/e* 775.4.

(*S,R*)-BPPFAP-BPh-Cl (3c). (*S,R*)-BPPFAP (86 mg, 0.125 mmol) and ClPhB(O) (100 mg, 0.72 mmol, 5.8 equiv) were reacted using the same conditions and workup as for **3a**. (4-Chlorophenyl)boric anhydride was prepared according to methods by Fields and Jacobsen.[7b] The crude product was recrystallized several times from diethyl ether (72 mg, 0.089 mmol, 71% yield). Anal. Calcd for $C_{48}H_{39}BNOP_2ClFe$: C, 71.18; H, 4.85; N, 1.73; P, 7.65; Cl, 4.38; Fe, 6.90. Found: C, 69.84; H, 6.19; N, 1.87; P, 6.28; Cl, 4.89; Fe, 6.62. $[\alpha]_D = +245$ ($CHCl_3$, $c = 0.39$). ^{1}H NMR ($CDCl_3$): δ 1.7 (d, $J = 7$ Hz, 3H, CHCH_3), 3.4−4.7 (7 peaks, m, 7H, $C_5H_3FeC_5H_4$), 5.7 (q, $J = 7$ Hz, 1H, CHCH$_3$), 6.4−8.0 ppm (m, 28H, BC_6H_4Cl, C_6H_4 and PC_6H_5). ^{31}P NMR ($CDCl_3$): δ −25.5 (s, C_5H_3P) and −17.4 ppm (s, C_5H_4P). LR LSIMS: M^+ at *m/e* 809.0.

Reactions of $PtMe_2$(COD) with *rac*-Phosphines 3a−c. A typical reaction was as follows: $PtMe_2$(COD) (19 mg, 1 equiv) and **3a** (41 mg, 1 equiv) were dissolved in 1 mL of C_6D_6 under N_2. The solution was heated to 60 °C for 30 min. Reactions were approximately 98% pure by ^{31}P NMR, where the impurity was attributed to trace PtMeI(L). Solvent and free COD were removed in vacuo.

$PtMe_2$(BPPFAP-BMe) (4a). ^{1}H NMR (C_6D_6): δ 0.69 (s, 3H, BCH_3), 0.72 (dt, 3H, $J_{Pt-H} = 35$ Hz, $J_{P-H} = 8$ Hz, Pt(CH_3)), 1.10 (dt, 3H, $J_{Pt-H} = 47$ Hz, $J_{P-H} = 8$ Hz, Pt(CH_3)), 1.20 (d, $J = 7$ Hz, 3H, CHCH_3), 3.25−4.19 (m, 7H, $C_5H_3FeC_5H_4$), 6.35−7.95 ppm (m, 25H, CHCH$_3$, C_6H_4NO and PC_6H_5). ^{31}P NMR (C_6D_6): δ 21.7 (dd, $J_{Pt-P} = 1841$ Hz, $J_{P-P} = 12$ Hz), 25.9 ppm (dd, $J_{Pt-P} = 1912$ Hz, $J_{P-P} = 12$ Hz). LR LSIMS: M^+ not present, $M^+ -$ Me at *m/e* 923.2.

$PtMe_2$(BPPFAP-BPh) (4b). ^{1}H NMR (C_6D_6): δ 0.82 (dt, 3H, $J_{Pt-H} = 35$ Hz, $J_{P-H} = 8$ Hz, Pt(CH_3)), 1.00 (dt, 3H, $J_{Pt-H} = 34$ Hz, $J_{P-H} = 8$ Hz, Pt(CH_3)), 1.72 (d, $J = 7$ Hz, 3H, CH$_3$), 3.02−3.74 (m, 7H, $C_5H_3FeC_5H_4$), 6.3−7.9 ppm (m, 30H, CHCH$_3$, C_6H_4NO, BC_6H_5, and PC_6H_5). ^{31}P NMR (C_6D_6): δ 22.1 (dd, $J_{Pt-P} = 1829$ Hz, $J_{P-P} = 12$ Hz), 26.3 ppm (dd, $J_{Pt-P} = 1912$ Hz, $J_{P-P} = 12$ Hz). LR LSIMS: M^+ at *m/e* 1000.1 (very weak), $M^+ -$ Me at *m/e* 985.1.

$PtMe_2$(BPPFAP-BPhCl) (4c). ^{1}H NMR (C_6D_6): δ 0.82 (dt, 3H, $J_{Pt-H} = 26$ Hz, $J_{P-H} = 8$ Hz, Pt(CH_3)), 1.29 (dt, 3H, $J_{Pt-H} = 35$ Hz, $J_{P-H} = 8$ Hz, Pt(CH_3)), 1.37 (d, $J = 7$ Hz, 3H, CHCH_3), 3.01−4.10 (m, 7H, $C_5H_3FeC_5H_4$), 6.3−7.9 ppm (m, 29H, CHCH$_3$, C_6H_4NO, C_6H_4Cl, and PC_6H_5). ^{31}P NMR (C_6D_6): δ 22.8 (dd, $J_{Pt-P} = 1829$ Hz, $J_{P-P} = 12$ Hz), 26.2 ppm (dd, $J_{Pt-P} = 1905$ Hz, $J_{P-P} = 12$ Hz). LR LSIMS: M^+ at *m/e* 1020.2.

Reaction of $PtMe_2$(COD) with *rac*-BPPFAP (2). $PtMe_2$(COD) (20 mg, 0.060 mmol) and **2** (42 mg, 0.061 mmol, 1.02 equiv) were dissolved in acetone (10 mL) under N_2. A small amount of yellow solid came out of solution. The mixture was filtered, and the filtrate was determined to be a mixture of several unknown species. The trace amount of pale yellow solid was dissolved and found to be pure product. The product decomposed slowly in solution under N_2 and in the absence of light. ^{1}H NMR ($CDCl_3$): δ 0.24 (dt, 3H, $J_{Pt-H} = 38$ Hz, $J_{P-H} = 8$ Hz, Pt(CH_3)), 0.59 (dt, 3H, $J_{Pt-H} = 34$ Hz, $J_{P-H} =$ Hz, Pt(CH_3)), 1.21 (d, $J = 6$ Hz, 3H, CHCH_3), 3.52−4.48 (m, 7H, $C_5H_3FeC_5H_4$), 5.99 (q, $J = 6$ Hz, 1H, CHCH$_3$), 6.58−7.87 ppm (m, 24H, C_6H_4NO and PC_6H_5). ^{31}P NMR (C_6D_6): δ 20.07 (dd, $J_{Pt-P} = 1829$ Hz, $J_{P-P} = 8$ Hz), 25.89 ppm (dd, $J_{Pt-P} = 1918$ Hz, $J_{P-P} = 8$ Hz).

PtMeI(*rac*-BPPFAP) (5a,b). A solution of *rac*-**2** (160 mg, 0.23 mmol, 1.0 equiv) in THF (5 mL) was added to a THF (5 mL) solution of PtMeI(COD) (103 mg, 0.23 mmol, 1.0 equiv) in a Schlenk flask under N_2. The solution was filtered and the yellow solid was recrystallized from Et_2O/THF (154 mg, 0.15 mmol, 65% yield). All manipulations were done under N_2 and in the absence of light. [PtMeI(BPPFAP)] was found to be an approximately 1:1 mixture of two isomers by ^{31}P NMR. **5a**: ^{31}P NMR (C_6D_6) δ 22.8 (dd, $J_{Pt-P} = 1926$ Hz, $J_{P-P} = 12$ Hz), 16.6 (dd, $J_{Pt-P} = 4282$ Hz, $J_{P-P} = 12$ Hz); **5b**: ^{31}P NMR (C_6D_6) δ 19.5 (dd, $J_{Pt-P} = 4255$ Hz, $J_{P-P} = 12$ Hz), 15.4 ppm (dd, $J_{Pt-P} = 1856$ Hz, $J_{P-P} = 12$ Hz). ^{1}H NMR (C_6D_6): too complicated to interpret due to overlap of the two isomers. LR LSIMS: M^+ at *m/e* 1025.8.

Structure Determination of *rac*-5. A single crystal was grown from THF/diethyl ether at 0 °C. Crystal data are summarized in Table 4.

A total of 16 594 reflections with $2\theta < 52.1°$ were collected on a Siemens P4/CCD diffractometer using graphite-monochromated Mo Kα radiation.[20] The structure was solved by direct methods and was refined by full-matrix least squares on F^2 values with hydrogens riding.[19] Non-hydrogen atoms were refined with anisotropic thermal parameters. The final $R(F)$ and $R_w(F^2)$ factors were 0.027 and 0.076, respectively. A molecular structure is shown in Figure 4, along with a partial numbering scheme. Selected bond lengths and bond angles are given in Table 3. Fractional coordinates and additional crystallographic data can be found in the Supporting Information.

[Rh(NBD)(BPPFAc)]OTf (7). [Rh(NBD)$_2$]OTf (68.0 mg, 0.157 mmol, 1.00 equiv) and (*S,R*)-BPPFAc (102 mg, 0.159 mmol, 1.01 equiv) were placed in a Schlenk flask under nitrogen with 5 mL of freshly distilled THF. The bright red solution was stirred for 30 min, and the solvent volume was reduced to approximately 2 mL and layered with 4 mL of diethyl ether. The mixture was filtered yielding a red-orange solid (102 mg, 0.104 mmol, 66% yield). ^{1}H NMR (acetone-d_6): δ 1.56 (s, 2H, CH_2 of NBD), 1.92 (s, 3H, COCH_3), 2.07 (d, $J =$ 6 Hz, 3H, CHCH_3), 3.78−5.66 (m, 14H, CHCH$_3$, $C_5H_3FeC_5H_4$ and remaining NBD), 6.56−7.04 (m, 4H, C_6H_4NO), 7.0−8.3

(20) Data collection and reduction: (a) *SMART Software Reference Manual*; Siemens Analytical X-ray Instruments: Madison, WI, 1994. (b) *SAINT Version 4 Software Manual*; Siemens Analytical X-ray Instruments: Madison, WI, 1995.

ppm (m, 20H, PC_6H_5). ^{31}P NMR (acetone-d_6): δ 26.0 (dd, J_{Rh-P} = 161 Hz, J_{P-P} = 26 Hz), 28.9 ppm (dd, J_{Rh-P} = 161 Hz, J_{P-P} = 26 Hz). LR LSIMS: M^+ = [Rh(NBD)(**1**)]$^+$ at *m/e* 835.2.

[Rh(NBD)(BPPFAP)]OTf (8). [$Rh(NBD)_2$]OTf (63.3 mg, 0.145 mmol, 1.00 equiv) and (*S,R*)-**2** (102 mg, 0.148 mmol, 1.02 equiv) was reacted as above. The product was crystallized from THF/diethyl ether yielding a red powder, **8** (88 mg, 0.085 mmol, 59%). Small amounts (approximately 5%) of an impurity were consistently found in the isolated product (^{31}P NMR (acetone-d_6): δ 17.85 (d, J_{Rh-P} = 159 Hz), 22.1 ppm (d, J_{Rh-P} = 167 Hz)). ^1H NMR (acetone-d_6): δ 1.48 (s, 2H, CH_2 of NBD), 1.81 (d, J = 7 Hz, 3H, $CHCH_3$), 4.01−5.08 (7 peaks, m, 13H, $C_5H_3FeC_5H_4$ and remaining NBD), 5.69 (q, J = 7 Hz, 1H, $CHCH_3$), 6.56−7.04 (m, 4H, C_6H_4NO), 7.1−8.4 ppm (m, 20H, PC_6H_5). ^{31}P NMR (acetone-d_6): δ 26.8 (dd, J_{Rh-P} = 159 Hz, J_{P-P} = 27 Hz), 31.4 ppm (dd, J_{Rh-P} = 160 Hz, J_{P-P} = 27 Hz). LR LSIMS: M^+ = [Rh(NBD)(**2**)]$^+$ at *m/e* 884.3.

[Rh(NBD)(BPPFAP-BMe)]OTf (9). [$Rh(NBD)_2$]OTf (61.2 mg, 0.140 mmol, 1.00 equiv) and (*S,R*)-**3a** (102 mg, 0.143 mmol, 1.02 equiv) were reacted by following the procedure for **7**. The product was crystallized from THF/diethyl ether, yielding a red powder, **9** (112 mg, 0.106 mmol, 76%). ^1H NMR (acetone-d_6): δ 0.26 (s, 3H, BCH_3), 1.46 (d, J = 7 Hz, 3H, $CHCH_3$), 1.54 (m, 2H, CH_2 of NBD), 3.95−5.12 (8 peaks, m, 13H, $C_5H_3FeC_5H_4$ and NBD), 5.03 (q, J = 7 Hz, 1H, $CHCH_3$), 6.91−7.35 (m, 4H, C_6H_4NO), 7.40−8.10 ppm (m, 20H, PC_6H_5). ^{31}P NMR (acetone-d_6): ABX pattern, δ 22.1 (J_{Rh-P} = 163 Hz, J_{P-P} = 25 Hz), 26.3 ppm (J_{Rh-P} = 160 Hz). LR LSIMS: M^+ = [Rh(NBD)(**3a**)]$^+$ at *m/e* 908.2.

Reactions of [$Rh(NBD)_2$]OTf with Ligands 3b,c. A typical reaction was as follows: a solution of *rac*-**3b** (18.5 mg, 0.024 mmol, 1 equiv) in THF was added to a THF solution of[$Rh(NBD)_2$]OTf (10.4 mg, 0.024 mmol, 1 equiv). All manipulations were done under N_2, and a total volume of 1 mL of freshly distilled THF was used. The reactions were followed by ^{31}P NMR.

Reaction of [$Rh(NBD)_2$]OTf with 3b. Initially a single product, exhibiting shifts in solution similar to those for complex **3a**, was formed (^{31}P NMR (THF): δ 27.11 (br dd, J_{Rh-P} = 170 Hz, J_{P-P} = 24 Hz), 28.38 ppm (dd, J_{Rh-P} = 162 Hz, J_{P-P} = 25 Hz)). This complex slowly decomposed ($t_{1/2}$ = approximately 3 days) to a single new species. Attempts to isolate the desired product by using the procedure for **7** resulted in exclusive formation of the above-mentioned species, which has defied characterization.

Reaction of [$Rh(NBD)_2$]OTf with 3c. Initially a single product, exhibiting shifts in solution similar to those for complex **3a**, was formed (^{31}P NMR (THF): δ 27.07 (br dd, J_{Rh-P} = 160 Hz, J_{P-P} = 26 Hz), 28.73 ppm (dd, J_{Rh-P} = 163 Hz, J_{P-P} = 26 Hz)). This complex slowly decomposed ($t_{1/2}$ = approximately 3 days) to a single new species. Attempts to isolate the desired product by using the procedure for **7** resulted in formation of a 1:1 mixture of desired product and unknown species, which has defied characterization.

Hydrogenation of MAC. For hydrogenations using ligands **1**, **2**, and **3a**, the isolated [Rh(NBD)(L)]OTf complex **7**, **8**, or **9** (0.8 mM) was dissolved in freshly distilled THF and 400 equiv of MAC was added. For hydrogenations using ligands **3b**,**c**, a 1:1 mixture of [$Rh(NBD)_2$]OTf (0.8 mM) and the phosphine (**3b** or **3c**) was dissolved in freshly distilled THF; 400 equiv of MAC was added. All hydrogenations were run in pressure bottles at 15 psig of H_2 and 22 °C. Rates were monitored by ^1H NMR, and enantiomeric excesses were determined by GC on a Chirasil-Val column.

Hydroformylation of Styrene. A 4:1 mixture of phosphine **1**, **2**, or **3** and Rh(acac)$(CO)_2$ was dissolved in freshly distilled THF. The reactions were run at a pressure of 90 psig of 1:1 CO:H_2 and Rh(acac)$(CO)_2$ concentration of 0.6 mM. Styrene (120 equiv) was added after a 1 h incubation period. All reactions were followed by GC on a methyl silicone column. Initial turnover (to) frequencies of the various ligands at 2 h of reaction time and i:n aldehyde ratios were as follows: **1**: 12 to/h (i:n = 2); **2**: 7 to/h (i:n = 4); **3a**: 6 to/h (i:n = 4); **3b**: 6 to/h (i:n = 5); **3c**: 13 to/h (i:n = 4).

Acknowledgment. This work was supported by the Department of Energy, Office of Basic Energy Service (Contract No. DE-FG02-95ER14532). The Department of Chemistry Instrument Center is supported by the University of Wisconsin and the National Science Foundation.

Supporting Information Available: Figures giving additional views of the structure and unit cell and tables of fractional coordinates, thermal parameters, and bond lengths and angles (complete) for **2**, **3a**, and **5** (28 pages). Ordering information is given on any current masthead page.

OM960447+